Science Advances
AAAS

advances.sciencemag.org/cgi/content/full/5/11/eaax7256/DC1

Supplementary Materials for

Fast surface dynamics enabled cold joining of metallic glasses

Jiang Ma, Can Yang, Xiaodi Liu, Baoshuang Shang, Quanfeng He, Fucheng Li, Tianyu Wang, Dan Wei, Xiong Liang, Xiaoyu Wu, Yunjiang Wang, Feng Gong*, Pengfei Guan*, Weihua Wang*, Yong Yang*

*Corresponding author. Email: gongfeng@szu.edu.cn (F.G.); pguan@csrc.ac.cn (P.G.); whw@iphy.ac.cn (W.W.); yonyang@cityu.edu.hk (Y.Y.)

Published 22 November 2019, *Sci. Adv.* **5**, eaax7256 (2019)
DOI: 10.1126/sciadv.aax7256

The PDF file includes:

Other Supplementary Material for this manuscript includes the following:

(available at advances.sciencemag.org/cgi/content/full/5/11/eaax7256/DC1)

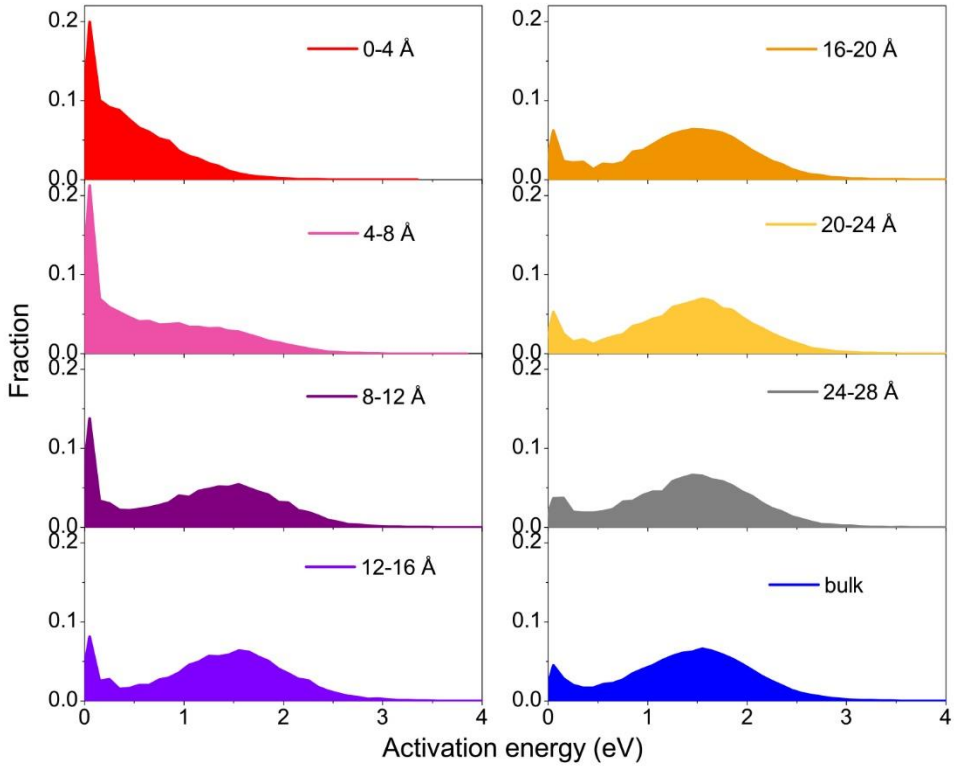

Fig. S1. Evolution of activation energy with the distance away from surface.

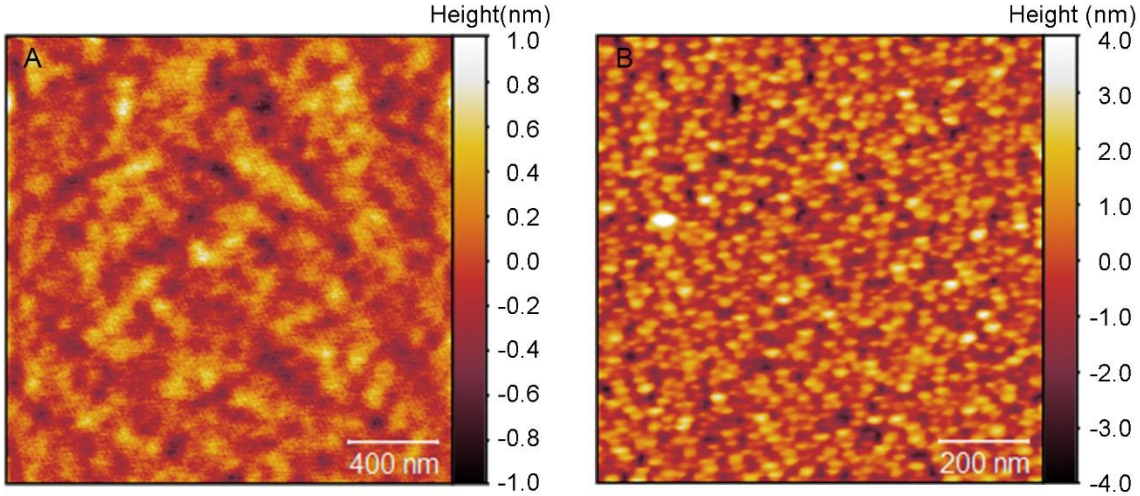

Fig. S2. Topology of the metallic glass thin films, which corresponds to the regions in Fig. 3 (A and B).

Fig. S3. Top views of the three metallic glass ribbons and the corresponding BMGs fabricated by the ultrasonic vibration method. (Photo credits: Dr. J. Ma, Shenzhen University)

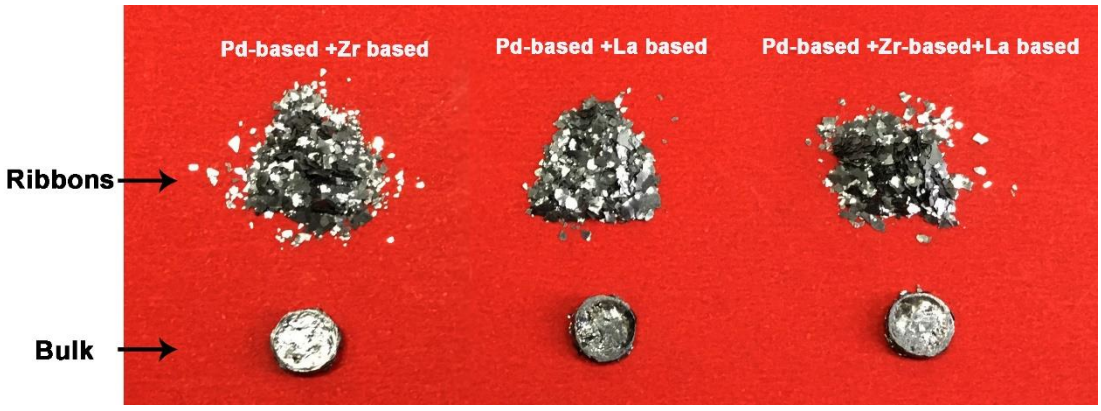

Fig. S4. The top views of the samples with dual phases of Zr-Pd BMG, Pd-La BMG, and even the ternary Zr-Pd-La BMG with a diameter of 5 mm. (Photo credits: Dr. J. Ma, Shenzhen University)

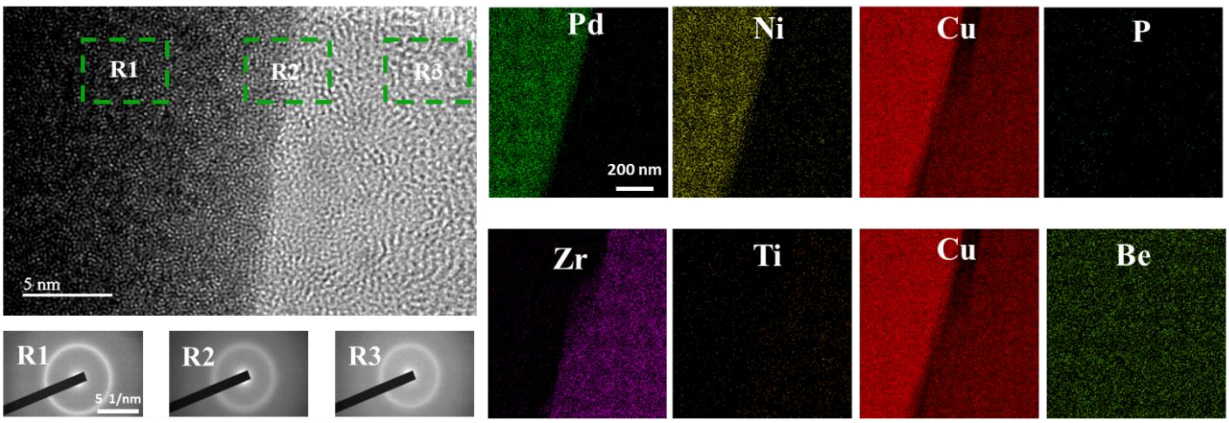

Fig. S5. The HRTEM image of the Pd-based and Zr-based dual-phase BMG and the corresponding element distribution. Three diffraction patterns share the same scale bar of 5 1/nm while eight element distribution maps share the same scale bar of 200 nm.

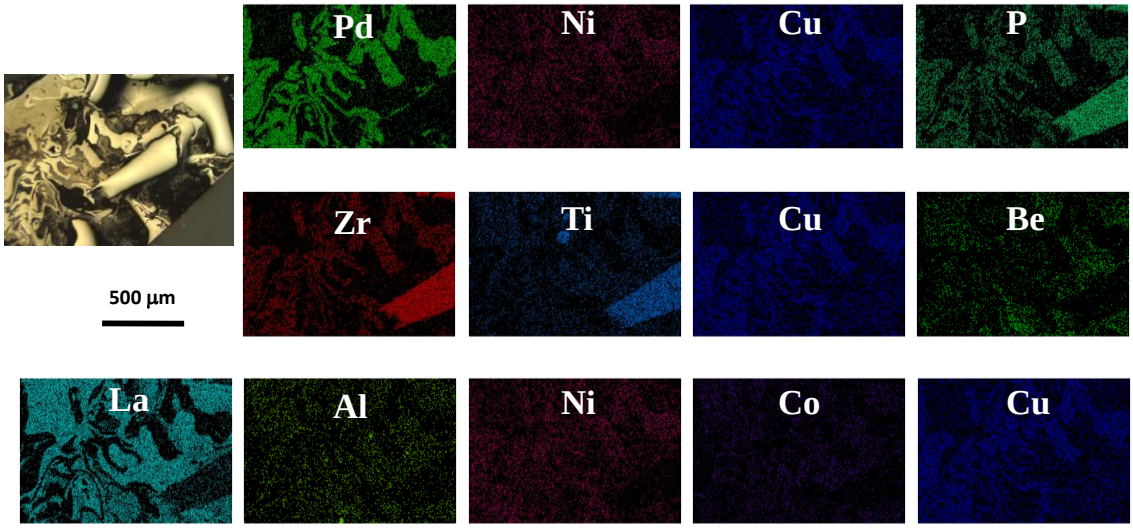

Fig. S6. The optical image of the Pd-, Zr-, and La-based multiphase BMG and the corresponding element distribution. All the images share the same scale bar.

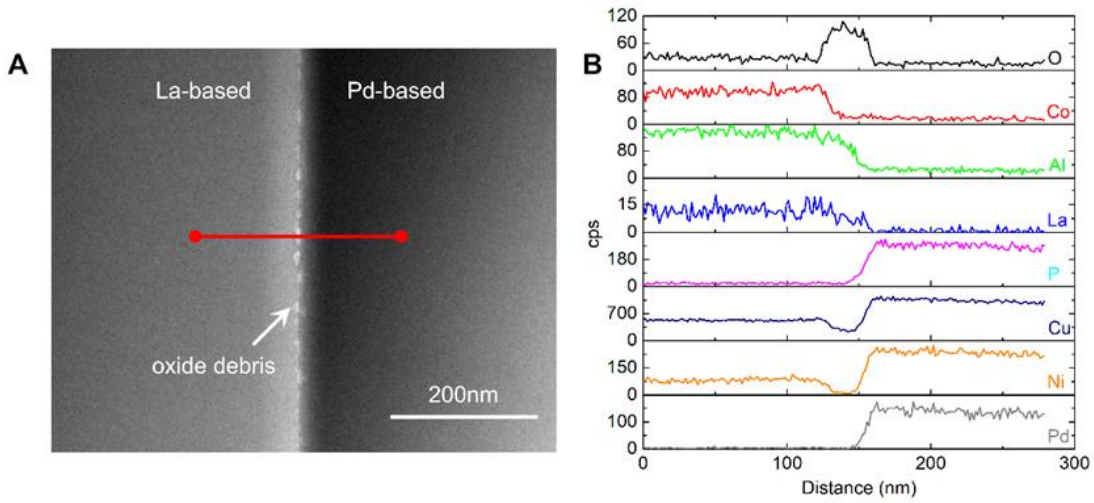

Fig. S7. The characterization of La-based and Pd-based dual-phase BMG interface. (**A**) The TEM image of the La-based and Pd-based dual phase BMG interface. It shows that the surface oxide layer has been broken into small pieces. (**B**) The EDS line scanning results of constituent elements along the dual phase BMG interface. The red line in (A) indicates the line scan position.

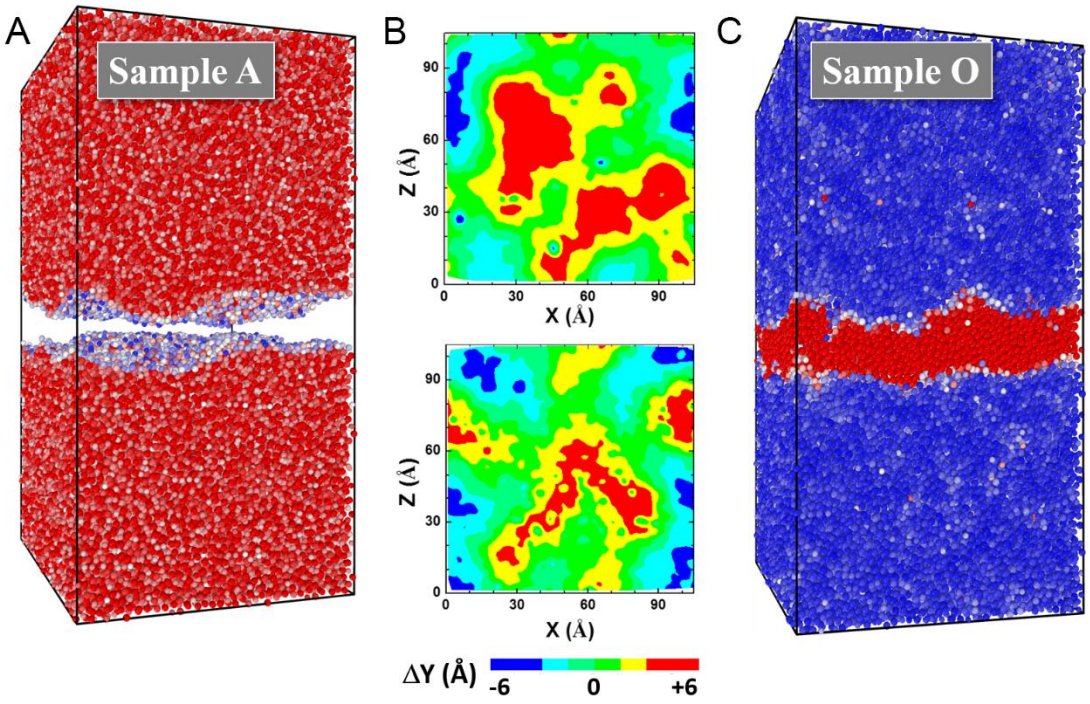

Fig. S8. Sample model preparation for MD simulations. (**A**) Two rough surfaces were constructed by deleting the atoms in the middle. (**B**) Roughness maps of two surfaces. (**C**) Sample model with pre-seeded interface.

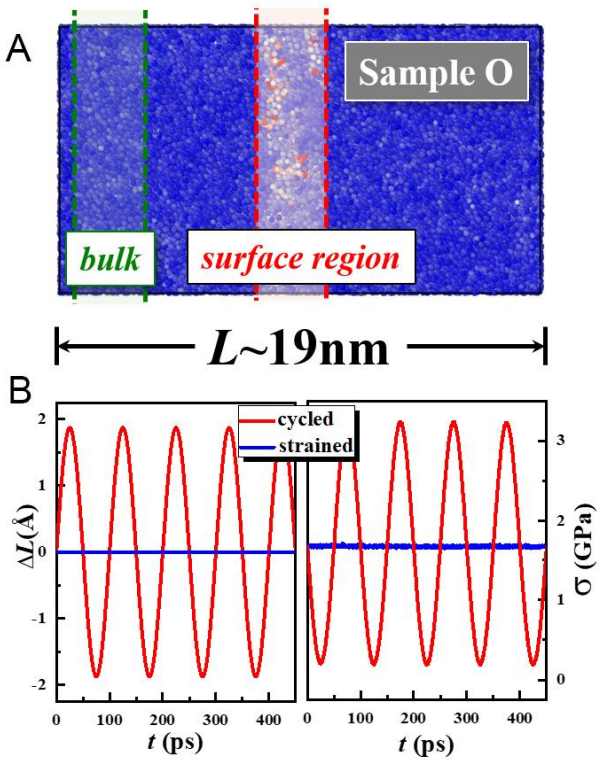

Fig. S9. Mechanical training on sample O. (**A**) Surface and bulk region in sample O. (**B**) Change in length ΔL and stress σ variation during the constant-strain training method (blue curves) and constant-frequency vibration method (red curves).

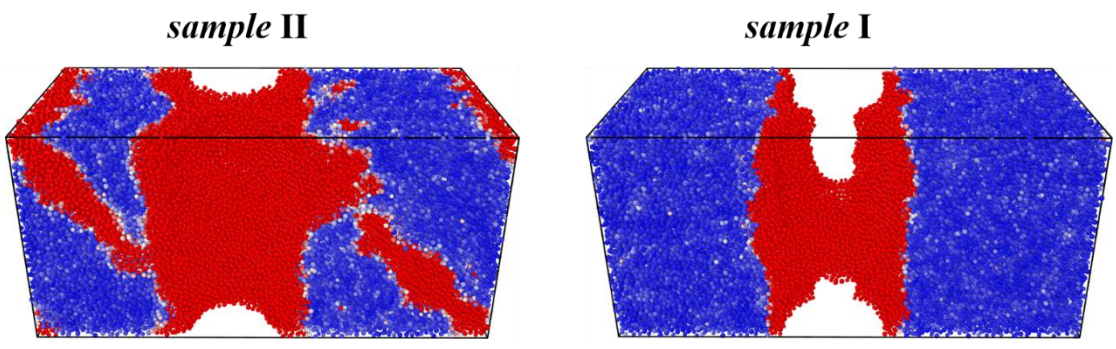

Fig. S10. Nonaffine displacement of each atom after applying the uniaxial tension.